PROCEEDINGS OF SCIENCE

Error mitigation strategies for simple quantum systems

K. Zambello,[a,*] **M. D'Elia**[a] **and R. Pariente**[a]

[a] *Università di Pisa and INFN, Sezione di Pisa, Pisa, Largo B. Pontecorvo 3, I-56127 Pisa, Italy*

E-mail: kevin.zambello@pi.infn.it

Quantum hardware in the NISQ era suffers from noise, which affects the reliability and accuracy of quantum computation. Here we present a comparison of quantum error mitigation strategies for Hamiltonian simulation and variational quantum algorithms, using as test bench some simple fermionic systems and discrete gauge theories.

The 40th International Symposium on Lattice Field Theory (Lattice 2023)
July 31st - August 4th, 2023
Fermi National Accelerator Laboratory

[*] Speaker

PoS(LATTICE2023)221

1. Introduction

With the rapid development of quantum hardware we can start to explore the first applications of quantum computing algorithms to physics problems using real devices. Real-time dynamics [1], ground state calculations [2] and the calculation of thermal averages [3–6] are just a few examples of potential applications. Despite the intriguing prospects for this emerging new technology, quantum computers in the current noisy intermediate-scale quantum (NISQ) era suffer from noise which hampers the accuracy and reliability of the calculations. In this work we compare different error mitigation strategies using some simple quantum systems as test bench.

2. Error mitigation strategies

We can categorize quantum error mitigation strategies into two classes. There are approaches that aim to mitigate the noise that comes from specific quantum error channels and agnostic approaches that do not strictly depend on the nature of the noise that affects the system. Here we focus on one method that belongs to the first type, i.e. global depolarizing noise mitigation and three methods that belong to the second type, i.e. zero-noise extrapolation, measurement error mitigation and general error mitigation.

2.1 Zero noise extrapolation

In zero noise extrapolation (ZNE) [7–9] one runs N copies of the original circuit where the noise has been increased by N factors $\{\lambda_i\}_{i=1}^N$. The noise can be increased by unitary folding: given a circuit C with gate decomposition $C = U_M \dots U_0$, a subset of the circuit gates $\{U_j\}$ is replaced by $U_j \mapsto (U_j U_j^\dagger)\, U_j$. One obtains a circuit with more noise, but functionally equivalent to the original one. The ideal result $\langle O \rangle$ is estimated by extrapolating the noisy results $\{\langle O \rangle_i\}_{i=1}^N$ to the $\lambda \to 0$ limit.

2.2 Measurement error mitigation and general error mitigation

Measurement error mitigation (MEM) [10] mitigates readout noise, which is the dominant source of noise for very short circuits. The mitigation is done using a calibration matrix such that

$$\vec{f}_{noisy} = M\, \vec{f}_{ideal}\ , \tag{1}$$

where $\vec{f}_{ideal}$ are the ideal count probabilities and $\vec{f}_{noisy}$ are the count probabilities that are actually measured in the presence of noise. The i-th column of M is estimated by the count probabilities of a measurement taken just after preparing the state $|i\rangle$. Once M is known, the noisy results $\vec{f}_{noisy}$ from a measurement done after the execution of a generic circuit can be mitigated by minimizing $||M\vec{x} - \vec{f}_{noisy}||_2^2$ while imposing the normalization condition $\sum_i x_i = 1$ and positive definiteness condition $x_i \in [0, 1]$.

General error mitigation (GEM) [11] generalizes measurement error mitigation to take into account gate noise. This is done heuristically. The original circuit C is split into two parts having (approximately) equal depth, $C^{(1)}$ and $C^{(2)}$, and two calibration circuits are built out of these, $C^{(1)}_{calib} = C^{(1)\dagger}\, C^{(1)}$ and $C^{(2)}_{calib} = C^{(2)\dagger}\, C^{(2)}$. These circuits are functionally equivalent to the

identity and carry information about the noise from the first and second half of the original quantum circuit. For each calibration circuit, one builds the associated calibration matrix following the same procedure as in MEM: initialize the system to the state $|i\rangle$, then apply the calibration circuit and finally measure. The count probabilities are estimates for the entries of the i-th column of the calibration matrix. At the end one has two calibration matrices that are averaged to get the calibration matrix that is actually used for the mitigation.

Given an N-qubits circuit these methods require the execution of respectively 2^N and $2 \cdot 2^N$ mitigation runs and the computational cost of mitigation scales exponentially with the number of qubits. This cost can be lowered assuming that qubits are affected by uncorrelated noise. In this case a $2^N \times 2^N$ calibration matrix $M = Q_{N-1} \otimes Q_{N-2} \otimes \ldots \otimes Q_1 \otimes Q_0$ is built by tensoring N 2×2 calibrations matrices Q_j tailored to the individual qubits. As for GEM one actually builds two calibration matrices, one for each half of the original circuit, and takes the average of these two. The matrices Q_j are constructed using the same calibration circuits used for GEM, $C^{(1)}_{calib} = C^{(1)\dagger}\, C^{(1)}$ and $C^{(2)}_{calib} = C^{(2)\dagger}\, C^{(2)}$. For every qubit j one sets the initial state to $|0\rangle_{N-1} \otimes \ldots \otimes |0\rangle_{j+1} \otimes |i\rangle_j \otimes |0\rangle_{j-1} \otimes \ldots \otimes |0\rangle_0$, then executes the calibration circuit and finally measures the j-th qubit. The count probabilities estimate the entries of the i-th column of Q_j. This tensored version of general error mitigation (TGEM) requires the execution of $2 \cdot 2N$ calibration circuits.

2.3 Global depolarizing noise mitigation

Assuming that the dominant noise in a quantum circuit is that of an effective depolarising error channel that with probability p replaces the quantum state with the maximally mixed state,

$$\mathcal{E}(\rho) = (1-p)\rho + \frac{p}{2^N}\,\mathbb{I}_{2^N}\,,$$

the noisy expectation value of an observable O is given by

$$\begin{aligned}\langle O\rangle_{noisy} &= Tr[O\mathcal{E}(\rho)] = (1-p)Tr[O\rho] + \frac{p}{2^N}Tr[O] \\ &= (1-p)\langle O\rangle_{ideal} + \frac{p}{2^N}Tr[O].\end{aligned}$$

The ideal expectation value can be recovered from the depolarizing parameter p and the noisy expectation value using [12–14]

$$\langle O\rangle_{ideal} = \left(\langle O\rangle_{noisy} - \frac{p}{2^N}Tr[O]\right)(1-p)^{-1}\,. \tag{2}$$

Conversely the parameter p can be estimated using

$$p = \left(\langle O\rangle_{ideal} - \langle O\rangle_{noisy}\right)\left(\langle O\rangle_{ideal} - \frac{Tr[O]}{2^N}\right)^{-1},$$

where the noisy expectation value is measured after the execution of a calibration circuit affected by a noise similar to that of the original circuit but for which the ideal expectation value is known. In the case of Hamiltonian evolution, for instance, the evolution for $N/2$ Trotter steps of time step dt followed by $N/2$ Trotter steps of time step -dt can serve as the calibration circuit for the evolution for N Trotter steps of time step dt [14].

The effectiveness of global depolarising noise mitigation (DEP) can be increased with randomized compiling. In place of the original quantum circuit one executes N Pauli-twirled circuits, i.e. copies of the circuit where the CNOT gates have been replaced by random combinations of CNOT and 1-qubits gates (that are functionally equivalent to a CNOT gate). Randomized compiling is able to convert coherent noise into stochastic depolarizing noise [15] that can be mitigated using Eq. (2).

3. Applications

We applied these mitigation methods to Hamiltonian simulation and the Variational Quantum Eigensolver (VQE) [2] for some simple systems such as the two-sites Fermi-Hubbard model, the transverse-field Ising model on a square and the Z_2 gauge theory for a two-plaquettes system with both periodic and open boundary conditions. Along a similar line of work the application of quantum error mitigation to the simulation of the Z_2 gauge theory was also explored in Refs. [16, 17] for a $1d$ lattice.

3.1 Hamiltonian simulation

The two-sites Hubbard model describes interacting spin $1/2$ particles living on a two-sites lattice. The model is governed by the Hamiltonian

$$H = -t(c^\dagger_{0\uparrow}c_{1\uparrow} + c^\dagger_{1\uparrow}c_{0\uparrow} + c^\dagger_{0\downarrow}c_{1\downarrow} + c^\dagger_{1\downarrow}c_{0\downarrow}) + U(n_{0\uparrow}n_{0\downarrow} + n_{1\uparrow}n_{1\downarrow}) - \mu(n_{0\uparrow} + n_{0\downarrow} + n_{1\uparrow} + n_{1\downarrow}),$$

where $c_{i,s}$ are anti-commuting variables for the site i and spin s and $n_{is} = c^\dagger_{is}c_{is}$ is the occupation number. The model has been mapped to a quantum computer using a Jordan-Wigner transformation. The system is representable using 4 qubits and the evolution circuit is depicted in the left picture of Fig. 2. The circuit comprises 12 CNOT gates per Trotter step for fully connected qubits. On IBM quantum hardware the circuit uses 18 CNOTs per Trotter step due to the limited qubits connectivity which requires the execution of SWAP gates. The evolution has been run on `ibmq_kolkata` using 10000 shots. Numerical results for 2 and 4 Trotter steps are shown respectively in the top left and center left pictures of Fig. 1. The initial state has been set to $|n_{1\downarrow}\ n_{0\downarrow}\ n_{1\uparrow}\ n_{0\uparrow}\rangle = |1010\rangle$ and we measured the probability of observing a spin down particle at site 1. Unmitigated data are displayed in red. With 2 Trotter steps the evolution circuit is already deep enough that measurement error mitigation (magenta) has little effect. General error mitigation (blue), its tensored version (cyan) and global depolarizing noise mitigation combined with randomized compiling using 16 Pauli twirls (green) are effective in mitigating the errors. With 4 Trotter steps the noise increases; global depolarising noise mitigation still works reliably, while general error mitigation and its tensored version become less effective. The bottom left picture of Fig. 1 illustrates the results obtained by ZNE for 4 Trotter steps with a simulator using a noise model calibrated from `ibmq_kolkata`. Even on a noisy simulator it has proven difficult to keep under control the systematic uncertainty coming from the ansatz (linear, polynomial or exponential) chosen for extrapolating to the zero noise limit.

The transverse-field Ising model on a square is another system representable by 4 qubits. It is described by the Hamiltonian

$$H = J(\sigma^z_0\sigma^z_1 + \sigma^z_1\sigma^z_2 + \sigma^z_2\sigma^z_3 + \sigma^z_0\sigma^z_3) + h(\sigma^x_0 + \sigma^x_1 + \sigma^x_2 + \sigma^x_3). \tag{3}$$

The evolution circuit, depicted in the right picture of Fig. 2, has 8 CNOTs per Trotter step on ideal hardware and 14 CNOTs per Trotter step on IBM hardware. Numerical results are shown in the top right and center right picture of Fig. 1 for respectively 2 and 4 Trotter steps. The initial state has been set to $|0\rangle$ and the observable O is the local magnetization $\langle\sigma_0^z\rangle$. The evolution was run on *ibmq_kolkata* using 10000 shots. The overall picture is similar to the one we observed for the Hubbard model. With 2 Trotter steps all methods except measurement error mitigation are effective. For 4 Trotter steps global depolarising noise mitigation (with 16 Pauli twirls) is still able to mitigate the errors, but general error mitigation and its tensorised variant become ineffective. A possible explanation for the failure of GEM is the lack of randomized compiling. This was investigated by additional runs whose results are shown in the bottom right picture of Fig. 1. Indeed both GEM and TGEM, when combined with randomized compiling using respectively 8 and 16 Pauli twirls, are able to mitigate the errors, though this also increases the number of calibration circuits to run by a factor 8 and 16.

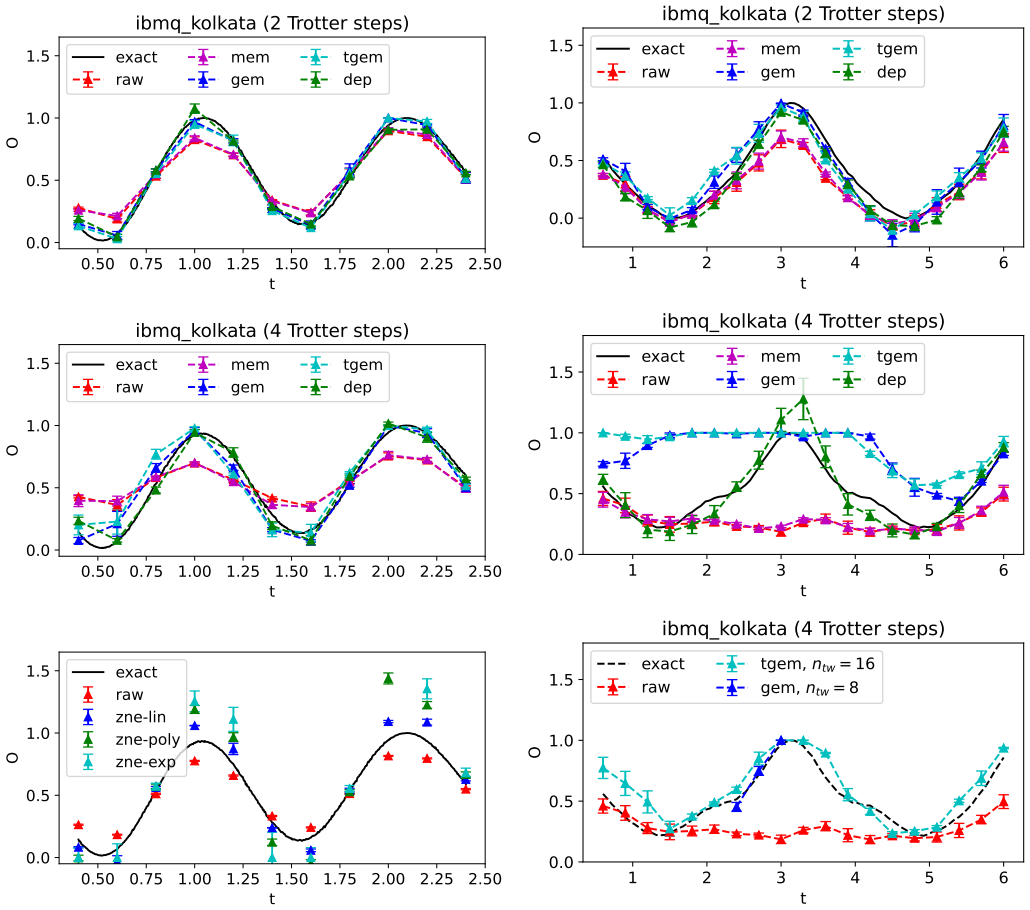

Figure 1: Two-sites Hubbard and 4-qubits Ising models: Hamiltonian simulation for 2 and 4 Trotter steps.

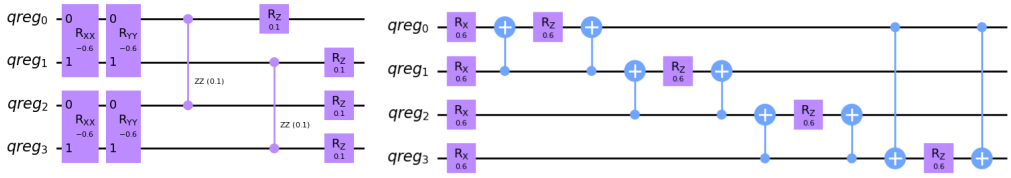

Figure 2: Two-sites Hubbard and 4-qubits Ising models: time evolution circuits.

For the Z_2 gauge theory we considered the two-plaquettes system depicted in the top left picture of Fig. 4, where lattice sites and gauge links are marked respectively by blue and green dots. With open boundary conditions (OBCs) the system is representable by 7 qubits, one for each link. When periodic boundary conditions (PBCs) are imposed, only 4 qubits are required. The Hamiltonians for open and periodic boundary conditions are respectively

$$H_{OBCs} = h(\sigma_0^x + \sigma_1^x + \sigma_2^x + \sigma_3^x + \sigma_4^x + \sigma_5^x + \sigma_6^x) + g(\sigma_0^z\sigma_1^z\sigma_2^z\sigma_3^z + \sigma_3^z\sigma_4^z\sigma_5^z\sigma_6^z) \,,$$

$$H_{PBCs} = h(\sigma_0^x + \sigma_1^x + \sigma_2^x + \sigma_3^x) + 2g\ \sigma_2^z\sigma_3^z \,.$$

The evolution circuits, shown in Fig. 3, comprise respectively 12 and 2 CNOTs per Trotter step. For both boundary conditions we used 10000 shots and we set the initial state to $|0\rangle$. Results are shown in Fig. 4. For PBC (top right picture) the evolution was done at constant $dt = 0.3$ and we measured the probability of observing the 0-th link in the state $|0\rangle$. Even for this very simple system omitting randomized compiling caused GEM and TGEM to fail and the only effective technique was global depolarizing noise mitigation (which was combined with 16 Pauli twirls). For OBC the evolution was done with 2 (bottom left) and 4 (bottom right) Trotter steps and we measured the probability of observing the 0-th link in the state $|0\rangle$. Overall global depolarizing noise mitigation (combined with 64 Pauli twirls) performed better than general error mitigation, though both were able to mitigate the errors only to some extent for 4 Trotter steps, where we observed cases of negative mitigation (i.e. unmitigated results being more accurate the mitigated results).

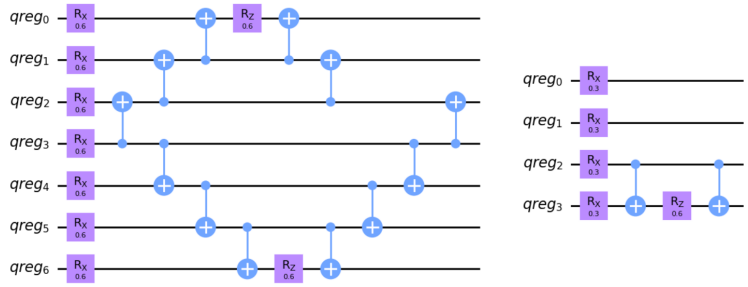

Figure 3: Z_2 gauge theory: time evolution circuits for a 2-plaquettes system with periodic (right) and open (left) boundary conditions.

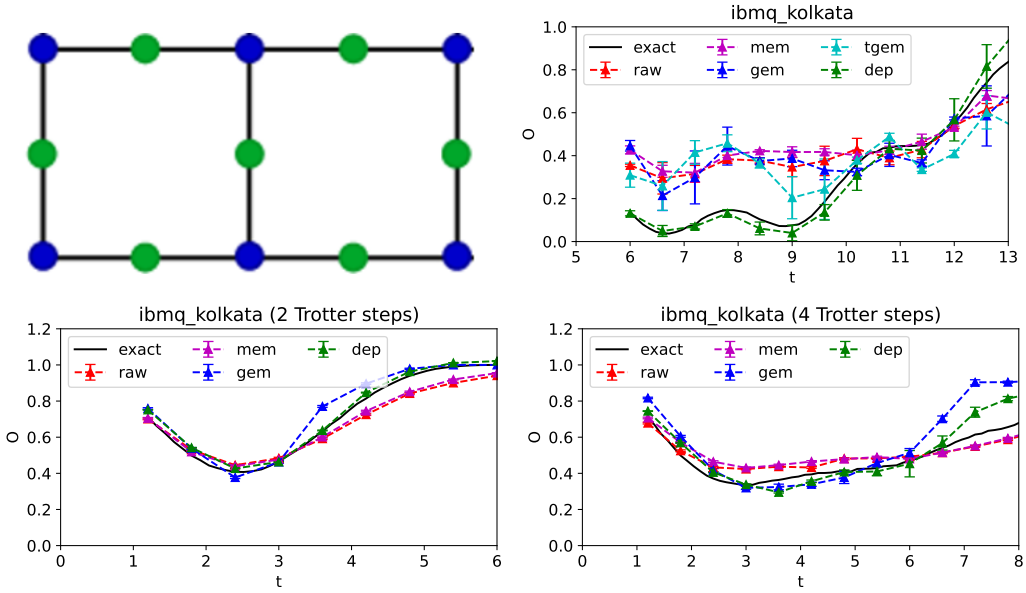

Figure 4: Z_2 gauge theory: Hamiltonian simulation for a 2-plaquettes system with periodic (top right) and open (bottom left and bottom right) boundary conditions. The evolution was done at fixed time step $dt = 0.3$ for PBC and at fixed number of Trotter steps $n_{trot} = 2$ (bottom left) and $n_{trot} = 4$ (bottom right) for OBC.

3.2 Variational Quantum Eigensolver

The Variational Quantum Eigensolver (VQE) [2] is a hybrid quantum-classical algorithm. It finds the ground state of a quantum system by parameterizing the state as $|\psi(\vec{\theta})\rangle = \prod_i U_i(\theta_i)|0\rangle$ and minimizing the cost function $\langle\psi(\vec{\theta})|\hat{H}|\psi(\vec{\theta})\rangle$, where $\hat{H}$ is the Hamiltonian. The minimization itself is done classically, while the cost function is evaluated on a quantum computer.

We tested the general error mitigation and global depolarizing noise mitigation techniques on the VQE for the Ising model and for the Z_2 gauge theory for a two-plaquettes system with open boundary conditions. We made use of 2-layers Hamiltonian ansätze, i.e. we expressed the parameterized state as $|\psi(\vec{\theta})\rangle = \left(\prod_{l=1}^{2}\left(\prod_{n=1}^{N} e^{-i\theta_{ln}\hat{H}_n}\right)\right)|\psi_0\rangle$ where $\hat{H}_n$ are the terms of the Hamiltonian and $|\psi_0\rangle$ is the eigenstate of a term of the Hamiltonian. For the initial state $|\psi_0\rangle$ we chose the ground state of the non-diagonal term of the Hamiltonian, which for both theories can be prepared using Hadamard gates.

We constructed the calibration circuits by splitting the quantum circuit that prepares the ansatz in half and composing each half with its own inverse. For GEM we obtain two calibration matrices that are averaged to get the one used for mitigation. Similarly, for DEP we obtain two depolarizing parameters and we use the average between the two to mitigate the errors. Fig. 5 illustrates the results obtained for the 2-qubits Ising model on `ibm_manila`. The left picture shows the results of the VQE with no mitigation, the center and right pictures show respectively the results obtained with GEM and DEP. The dashed line is the exact ground energy, while the blue (orange) data points are the energy expectation values measured (calculated exactly) for the (parameterized) quantum state at the given iteration of the VQE. General error mitigation and global depolarizing noise successfully mitigated the errors on the ground energy estimation, but notice that even the unmitigated VQE

was able to find the parameters corresponding to the ground state. The left and right pictures of Fig. 6 illustrate the results obtained with a noisy simulator for the 4-qubits Ising model and the Z_2 gauge theory. The blue, orange and green data are the energies measured at the given iteration of the VQE executed respectively with no mitigation, GEM/TGEM and DEP. Both GEM/TGEM and DEP were able to significantly reduce the noise bias.

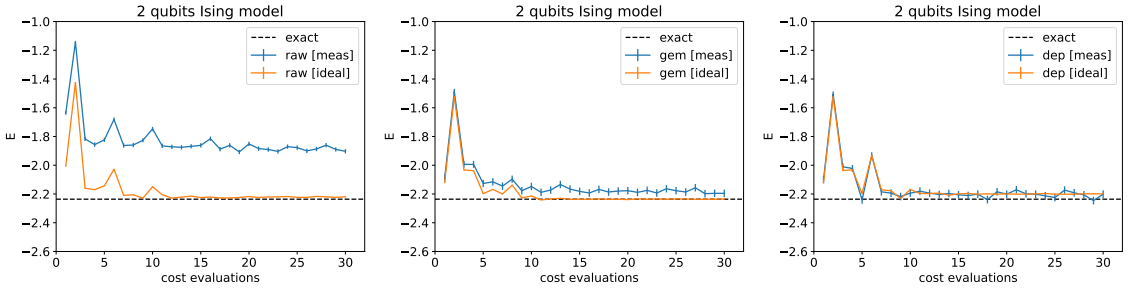

Figure 5: 2-qubits Ising model: calculation of the ground state using the VQE.

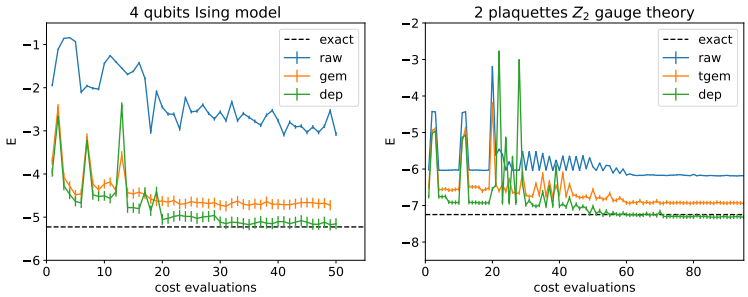

Figure 6: 4-qubits Ising model and Z_2 gauge theory for a two-plaquettes system: calculation of the ground state using the VQE.

4. Conclusions

We used and evaluated different quantum error mitigation methods for the Hamiltonian simulation of some simple quantum systems. The systematic of zero-noise extrapolation method was difficult to keep under control. Global depolarising error mitigation, combined with randomized compiling, was found to be a more reliable technique. For shallow circuits general error mitigation was also effective and we proposed a tensorised variant to make it more scalable with some trade-off on its effectiveness. For a successful application to deeper circuits, generalized error mitigation needs be combined with randomized compiling, though this raises the (already high) number of calibration circuits to run. Preliminary results show that general error mitigation and global depolarizing error mitigation can also be helpful for the Variational Quantum Eigensolver algorithm.

5. Acknowledgements

We thank C. Bonati, G. Clemente and L. Maio for useful discussions. This study was carried out within the National Centre on HPC, Big Data and Quantum Computing - SPOKE 10 (Quantum Computing) and received funding from the European Union Next-GenerationEU - National Recovery and Resilience Plan (NRRP) – MISSION 4 COMPONENT 2, INVESTMENT N. 1.4 – CUP N. I53C22000690001. Access to the IBM Quantum Services was obtained through the IBM Quantum Hub at CERN under the CERN-INFN agreement contract KR5386/IT and through the IBM Quantum Researchers Program. The research of K.Z. was funded by the University of Pisa under the PRA - Progetti di Ricerca di Ateneo (Institutional Research Grants) - Project No. PRA 2020-2021 92 "Quantum Computing, Technologies and Applications".

References

[1] Seth Lloyd, "*Universal Quantum Simulators*," Science **273**, 1073–1078 (1996).

[2] Alberto Peruzzo, Jarrod McClean, Peter Shadbolt, Man-Hong Yung, Xiao-Qi Zhou, Peter J. Love, Alán Aspuru-Guzik, and Jeremy L. O'Brien, "*A variational eigenvalue solver on a photonic quantum processor*," Nature Communications **5** (2014), 10.1038/ncomms5213.

[3] Giuseppe Clemente, "*Hybrid Quantum Estimation of Thermal Averages via Partial Mixed States Preparation*," PoS **LATTICE2023**, 216.

[4] Giuseppe Clemente, Marco Cardinali, Claudio Bonati, Enrico Calore, Leonardo Cosmai, Massimo D'Elia, Alessandro Gabbana, Davide Rossini, Fabio Sebastiano Schifano, Raffaele Tripiccione, and Davide Vadacchino, "*Quantum computation of thermal averages in the presence of a sign problem*," Physical Review D **101** (2020), 10.1103/physrevd.101.074510.

[5] Riccardo Aiudi, Claudio Bonanno, Claudio Bonati, Giuseppe Clemente, Massimo D'Elia, Lorenzo Maio, Davide Rossini, Salvatore Tirone, and Kevin Zambello, "*Quantum Algorithms for the computation of quantum thermal averages at work*," (2023), arXiv:2308.01279 [quant-ph] .

[6] Edoardo Ballini, Giuseppe Clemente, Massimo D'Elia, Lorenzo Maio, and Kevin Zambello, "*Quantum Computation of Thermal Averages for a Non-Abelian D_4 Lattice Gauge Theory via Quantum Metropolis Sampling*," (2023), arXiv:2309.07090 [quant-ph] .

[7] Kristan Temme, Sergey Bravyi, and Jay M. Gambetta, "*Error Mitigation for Short-Depth Quantum Circuits*," Phys. Rev. Lett. **119**, 180509 (2017), arXiv:1612.02058 [quant-ph] .

[8] Ritajit Majumdar, Pedro Rivero, Friederike Metz, Areeq Hasan, and Derek S. Wang, "*Best practices for quantum error mitigation with digital zero-noise extrapolation*," (2023), arXiv:2307.05203 [quant-ph] .

[9] Tudor Giurgica-Tiron, Yousef Hindy, Ryan LaRose, Andrea Mari, and William J. Zeng, "*Digital zero noise extrapolation for quantum error mitigation*," in *2020 IEEE International Conference on Quantum Computing and Engineering (QCE)* (IEEE, 2020).

[10] Filip B. Maciejewski, Zoltán Zimborás, and Michał Oszmaniec, "*Mitigation of readout noise in near-term quantum devices by classical post-processing based on detector tomography*," Quantum **4**, 257 (2020).

[11] Manpreet Singh Jattana, Fengping Jin, Hans De Raedt, and Kristel Michielsen, "*General error mitigation for quantum circuits*," Quantum Information Processing **19** (2020), 10.1007/s11128-020-02913-0.

[12] Joseph Vovrosh, Kiran E. Khosla, Sean Greenaway, Christopher Self, M. S. Kim, and Johannes Knolle, "*Simple mitigation of global depolarizing errors in quantum simulations*," Phys. Rev. E **104**, 035309 (2021).

[13] Miroslav Urbanek, Benjamin Nachman, Vincent R. Pascuzzi, Andre He, Christian W. Bauer, and Wibe A. de Jong, "*Mitigating Depolarizing Noise on Quantum Computers with Noise-Estimation Circuits*," Phys. Rev. Lett. **127**, 270502 (2021).

[14] Sarmed A Rahman, Randy Lewis, Emanuele Mendicelli, and Sarah Powell, "*Self-mitigating Trotter circuits for SU(2) lattice gauge theory on a quantum computer*," Physical Review D **106** (2022), 10.1103/physrevd.106.074502.

[15] Joel J. Wallman and Joseph Emerson, "*Noise tailoring for scalable quantum computation via randomized compiling*," Phys. Rev. A **94**, 052325 (2016).

[16] Clement Charles, Erik J. Gustafson, Elizabeth Hardt, Florian Herren, Norman Hogan, Henry Lamm, Sara Starecheski, Ruth S. Van de Water, and Michael L. Wagman, "*Simulating $\mathbb{Z}_2$ lattice gauge theory on a quantum computer*," (2023), arXiv:2305.02361 [hep-lat] .

[17] Henry Lamm, "*Simulating Z2 lattice gauge theory on a quantum computer*," PoS **LATTICE2023**, 218.